Cryst. Res. Technol., 1 – 6 (2009) / **DOI** 10.1002/crat.200900513

Quantification of the In-distribution in embedded InGaAs quantum dots by transmission electron microscopy

H. Blank*[1], D. Litvinov[1], R. Schneider[1], D. Gerthsen[1], T. Passow[2], and K. Scheerschmidt[3]

[1] Laboratorium für Elektronenmikroskopie and Center for Functional Nanostructures (CFN), Universität Karlsruhe (TH) / Karlsruhe Institut für Technologie (KIT), 76128 Karlsruhe, Germany
[2] Institut für Angewandte Physik und CFN, Universität Karlsruhe (TH) / Karlsruhe Institut für Technologie (KIT), 76128 Karlsruhe, Germany
[3] Max-Planck-Institut für Mikrostrukturphysik, 06120 Halle, Germany

Received 20 August 2009, accepted 24 August 2009
Published online 18 September 2009

Key words InGaAs quantum dots, In-distribution, TEM, CELFA.
PACS 81.07.Ta, 68.37.Lp, 68.37.Og

The In-concentration in InGaAs quantum dots located within a GaAs matrix was determined with the composition evaluation by lattice fringe analysis (CELFA) technique. However, the results obtained with this method cannot account for the three-dimensional shape of quantum dots and their embedding in GaAs. A correction procedure was developed that takes into consideration the shape of the quantum dots and the TEM sample thickness and quantum-dot size. After correction, In-concentration profiles show an increasing In-content towards the top of the quantum dots which is consistent with the effect of In-segregation and earlier studies using other experimental techniques.

Dedicated to Prof. Wolfgang Neumann on the occasion of his 65th birthday

1 Introduction

Self-assembled InGaAs quantum dots (QDs) in a GaAs matrix are of great interest because of many possible applications in optoelectronic devices (see, e.g., [1,2]). Owing to the growth by molecular beam epitaxy (MBE) in the Stranski-Krastanov growth mode, the In-concentration within a QD will be different from the nominal value. Usually, segregation effects cause an increase of the In-concentration towards the QD top [3,4]. As the optoelectronical properties strongly depend on the shape and composition of the QDs [5,6], these parameters have to be investigated. In transmission electron microscopy (TEM) the composition evaluation by lattice fringe analysis (CELFA) technique [7] has given valuable results for the composition determination in InGaAs quantum-well structures. However, applied to QDs within a host matrix this method alone cannot account for the three-dimensional shape of the QDs buried within the TEM sample. If the QDs are surrounded by a GaAs cap layer the measured In-concentration within the QDs will be too low due to an averaging effect along the thickness of the TEM specimen.

In this study a procedure is described to solve the averaging problem. Consequently, this correction procedure takes into consideration both the sample thickness and the QD shape, where the latter was determined by comparison of experimental plan-view bright-field (BF) images with simulated ones for QDs of different shapes and with further geometry information from cross-section high-angle annular dark-field (HAADF) scanning transmission electron microscopy (STEM) images. Together with the specimen thickness obtained by a tilt series of cross-section dark-field (DF) TEM images the initial CELFA results can be corrected.

* Corresponding author: e-mail: blank@lem.uni-karlsruhe.de

2 Experimental

The investigated samples were grown by MBE on a GaAs(001) substrate. The GaAs buffer with a thickness of 760 nm was deposited at a substrate temperature of 753 K followed by the deposition of 2.4 monolayers (ML) InAs at a deposition rate of 0.0057 ML/s. After an interruption time of 10 s a 28 nm thick GaAs capping layer was grown. TEM cross-section samples were prepared using standard procedures including ion milling [8]. Plan-view samples were prepared by chemical etching from the substrate side using a solution of NaOH (1mol/l) and H_2O_2 (30%) with a ratio of 5:1 to prevent the formation of additional defects. TEM micrographs were recorded using a Philips CM 200 FEG/ST electron microscope at 200 kV accelerating voltage. The In-concentration in the InGaAs layers was obtained on an atomic scale with CELFA. For this purpose, high-resolution TEM (HRTEM) lattice-fringe images were taken using [010] off-axis imaging conditions with a center of Laue circle (COLC) corresponding to (0,20,1.5) for imaging with the (002) reflection, whereas the COLC was (1.5,20,0) when the (200) reflection was used. In addition, HAADF STEM images were taken from InGaAs cross-section samples on a 200 kV LEO 922 Omega electron microscope using an electron probe of about 2 nm in diameter. Diffraction-contrast image simulations were performed for TEM bright-field imaging by using molecular-dynamically relaxed structure models of InAs QDs with different shapes and the EMS software package [9].

3 Results and discussion

The In-concentration in the region of InGaAs quantum dots formed during MBE growth was analyzed on an atomic scale with CELFA. For recording HRTEM lattice-fringe images an <100>-type zone-axis orientation was chosen, because the amplitude of the chemically sensitive {200} reflections is strongly affected by the {111} reflections in an <110>-type zone axis due to dynamical electron diffraction and nonlinear image formation in TEM. For simplicity, the following description focuses on imaging with the (200) reflection. Images with the (002) reflection were taken accordingly. The chemically sensitive (200) reflection was centered on the optical axis. Only the (000) beam and the (200) reflection were selected for the formation of lattice-fringe images. The local In-concentration is determined by measuring the amplitude of the (200) Fourier component of the image intensity and normalized with the amplitude of the (200) Fourier component from an adjacent region containing only GaAs. The local normalized (200) amplitudes are compared with (200) Fourier components calculated by the Bloch-wave method with structure factors which take also static atomic displacements into account (cf. [10] and references therein).

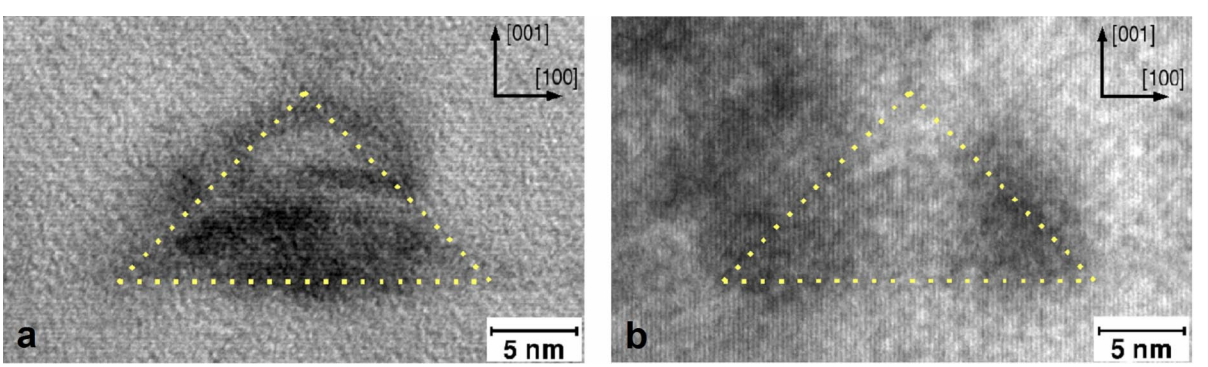

Fig. 1 TEM lattice-fringe images of a single InGaAs quantum dot obtained a) with the (000) and (002) reflections yielding (002) interference fringes perpendicular to the growth direction and b) with the (000) and (200) reflections yielding (200) interference fringes parallel to the growth direction. The position of the quantum dot is marked by a dashed line. (Online color at www.crt-journal.org)

Due to the strong bending of the (002) planes in the region of the QDs visible in figure 1a, strain contrast is superimposed on the lattice-fringe images. The bending of lattice planes leads to local deviations from the proper excitation conditions and consequently large errors in the CELFA evaluation. This is especially the case for micrographs recorded with the (002) reflection. For images taken with the (200) reflection (Fig. 1b) a

region in the center part of the QD between two dark lobes is observed with insignificant lattice plane bending and local deviations from the (200) excitation conditions. This region is suited for composition analysis.

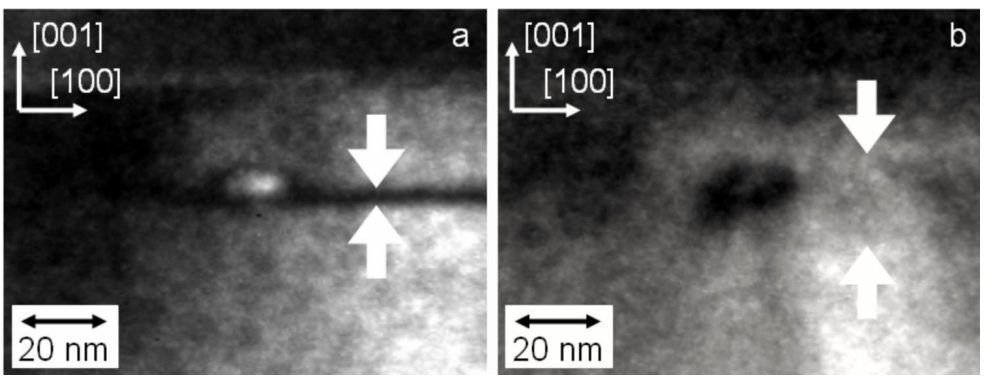

Fig. 2 (200) TEM dark-field images taken at tilt angles of a) 5° and b) 35°. The extent of the projected wetting layer is marked with arrows. It broadens with increasing tilt angle.

The local sample thickness was determined by recording of a tilt series of TEM DF images, where the chemically sensitive (200) beam was strongly excited. The sample was tilted around an axis parallel to the [100] direction in steps of 5° beginning close to the [010] zone axis. With increasing tilt angle the projection of the thin wetting layer broadens (cf. Fig. 2). By measuring the width w of the projected wetting layer at a given tilt angle α the local sample thickness can be calculated using simple trigonometry with the approximation of parallel surfaces of the sample. If the thickness of the wetting layer itself is small compared to the projected width, its dimension can be neglected and the sample thickness d is given by $d = w/\sin(\alpha)$. For the QD shown in figure 2 an averaged local sample thickness of 32 nm was obtained. Moreover, it can be deduced from the tilt series whether the QD is completely contained within the thin TEM sample or not. A QD only partially enclosed would be useless for further investigation since the determined In-concentration would always be too low. Such a cut-off QD can be identified through its relative position changes during the tilt series. If its position at high tilt angles moves from one boundary of the projected wetting layer to the other one, while going through the tilt angle of zero, it can be concluded that the QD is, at least, positioned close to a lateral surface of the sample and is likely contained only partially. The QD in figure 2 shows negligible position change and, hence, it is assumed that it is completely contained within the sample.

To determine the QD shape TEM BF images of a plan-view sample were recorded. In figure 3a InGaAs QDs with characteristic contrast are observed which can be compared with simulated images. The image simulations are based on InAs QD model structures with different shapes which are relaxed by molecular dynamics. Models were generated which contain QDs with hemispherical, {111}-, and {101}-facetted truncated pyramidal shape on an InAs wetting layer with 2 ML thickness. The whole structure is embedded in a GaAs matrix. Solving Newton's equations of motion by using suitably fitted many-body potentials, preferably of the empirical Tersoff or the semi-empirical Bond-Order type (cf. [11] and references therein), the prescribed geometric structures are relaxed applying annealing cycles up to 900 K.

The calculations are performed using mainly a Berendsen thermostat and for comparison also constant volume (NVE ensemble) or constant pressure (NpT ensemble) conditions, and time steps of the order of 0.25 fs. At each temperature step the QDs are relaxed for at least 10000 time steps. Nevertheless, the differences of the energy before and after relaxation is rather small, the different wetting layers, truncations, and stepping of facets yield characteristic strain fields. TEM BF images on the basis of the QD model structures were calculated in plan-view perspective applying the multislice formalism (Figs. 3b-d), where the relaxed supercells are sliced so that at least 4 subslices per unit cell in <100> direction are used.

The general contrast behavior of the simulated images of the {111}- and {101}-facetted truncated InAs pyramids (Figs. 3c,d) seems to be similar. However, both types of pyramids can be clearly differentiated by the orientation of their basal edges. Hence, by comparing the experimental images with simulated ones the presence of QDs in form of pyramids with {101} facets can be assumed. For the QDs investigated by CELFA this shape was also verified on cross-section specimens by means of HAADF STEM giving contrast that depends on the atomic number Z (Z-contrast) (see, e.g., [12]). In agreement with the {101}-facetted pyramids

these Z-contrast images (cf. Fig. 4) show pyramids with angles of around 45° between their sides and base. Moreover, the pyramids were found to be truncated.

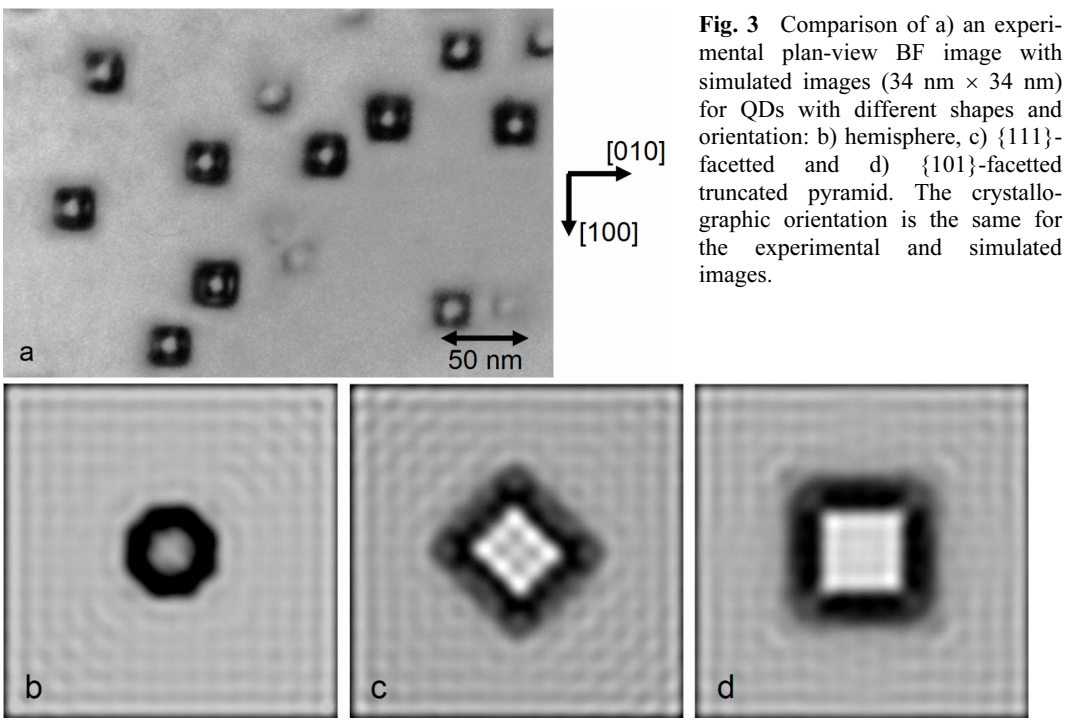

Fig. 3 Comparison of a) an experimental plan-view BF image with simulated images (34 nm × 34 nm) for QDs with different shapes and orientation: b) hemisphere, c) {111}-facetted and d) {101}-facetted truncated pyramid. The crystallographic orientation is the same for the experimental and simulated images.

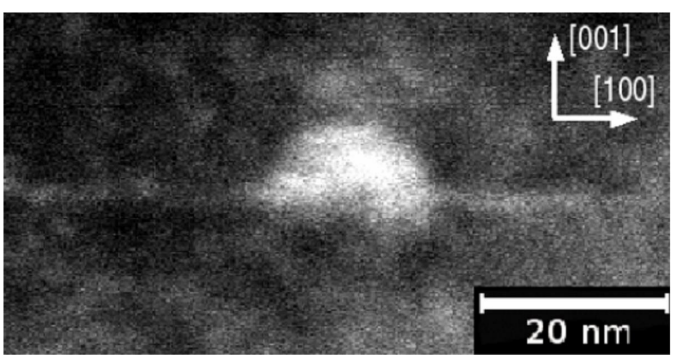

Fig. 4 HAADF STEM image of the InGaAs quantum dot under investigation. One and the same quantum dot was characterized by CELFA (see Figs. 5 and 6).

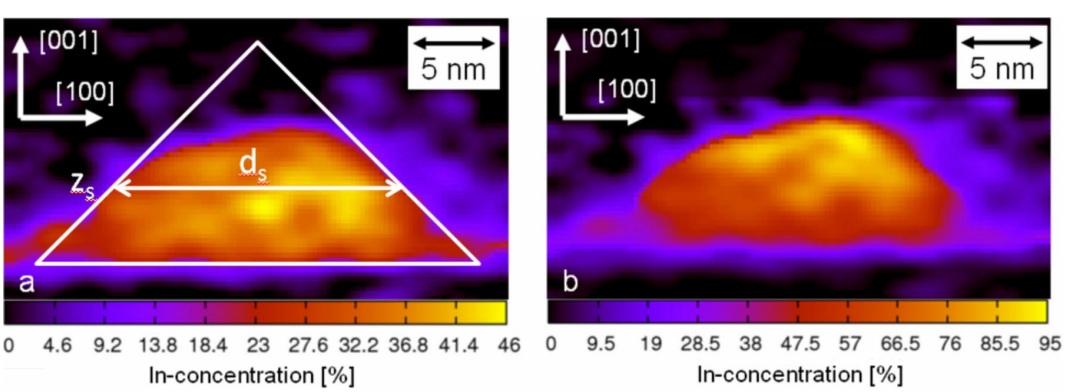

Fig. 5 Color-coded local In-concentration of a QD a) as obtained by CELFA with superimposed {101}-facetted pyramid and b) corrected In-concentration after post-processing.
(Online color at www.crt-journal.org)

Figure 5a shows a color-coded map of the local In-concentration of a QD obtained by CELFA. The In-concentration increases from the bottom and reaches a maximum value of 46 % in the center region of the QD. To correct the CELFA data for the above-mentioned thickness-dependent averaging effect, a projection of an {101}-facetted pyramid was fitted on the QD as shown in figure 5a. The relevant parameters for a correction are the distance d_S between the {101} facets and the vertical position z_S at which this distance is measured. The ratio V between the sample thickness d and the local thickness of the QD is then given as a function of the vertical coordinate z, i.e. $V(z) = d / (d_S + 2\cdot(z_S - z))$. Finally, multiplication of V with the local In-concentration obtained with the CELFA method yields the corrected In-concentration which takes into account the three-dimensional shape of the QD within the surrounding GaAs matrix and the sample thickness. The post-processing of the local In-concentrations in figure 5a, i.e. its multiplication with the ratio factor V, yields the corrected values shown in figure 5b. A maximal In-concentration of 95 % is found at the top of the QD. Obviously, the thickness correction also leads to a rearrangement of the In-distribution with the maximal In-content concentrated in the top region of the QD. The redistribution after correction is reasonable because the highest In-concentrations are expected close to the QD top due to the effect of In-segregation.

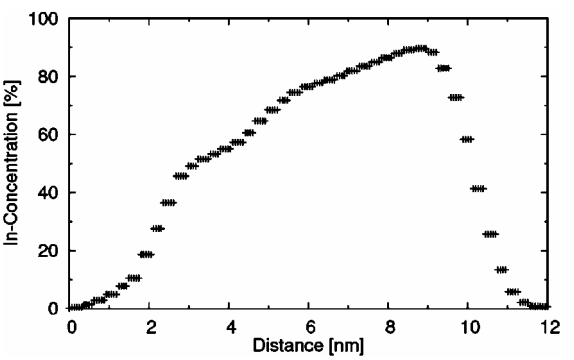

Fig. 6 In-concentration profile obtained by a 6 nm wide linescan as a function of distance in growth direction in the center of the InGaAs QD (cf. Fig. 5b).

This behavior can be also clearly seen in figure 6, showing the In-concentration profile as a function of the distance in growth direction which was obtained by averaging the In-concentration along a 6 nm wide linescan in the center of the QD from the base to the top. The In-concentration increases in the wetting layer and reaches about 50 % near the base of the QD. The In-concentration increases to almost 90 % at the top. This is in rather good agreement with earlier investigations on similar QDs by different methods like electron energy loss spectroscopy [13] and cross-sectional scanning tunneling microscopy [14].

Concerning the accuracy of the composition quantification it has to be taken into account that the QD shape can slightly deviate from the ideal shape of a {101}-facetted pyramid. This is especially a problem near the top of the QD, as the top is not truly flat. Furthermore, our correction procedure implies that the QD has the same shape and size in beam direction as it can be seen in the projection of the cross-section sample. If this is not the case, the fit of the ideal pyramid onto the projection leads to an error. An additional error is caused by the thickness measurement. The boundaries of the projected wetting layer at high tilt angles are not very sharp, causing an error in the width measurement and thus also in the determination of the thickness. With a more precise thickness determination and neglecting the fact that shape information of the third dimension for a specific QD is not accessible, the In-concentration should be measurable with a relative error of approximately 10 %.

4 Conclusion

For three-dimensional objects such as quantum dots embedded in a matrix with different composition, the measured concentrations for a quantum dot are inaccurate due to the averaging of the composition along the electron-beam direction. The evaluated composition depends on TEM sample thickness and object shape and size. This is demonstrated for InGaAs quantum dots with a base width of approximately 20 nm and 8 nm height grown on and capped with GaAs. Here, the originally measured In-concentration within the QDs is too low (maximal 46 %) due to averaging and the In-distribution is also affected. To correct for this effect a procedure was developed, where the ratio between TEM sample thickness and the local thickness of the QD must be known. The TEM sample thickness is obtained from tilt series of (200) DF TEM images. The QD

shape was determined by HAADF STEM imaging of cross-section samples and TEM BF images of plan-view samples. The latter were interpreted on the basis of simulated diffraction-contrast images which indicate that the InGaAs quantum dots occur with a shape of truncated pyramids with {101} facets. Taking the local thickness ratio and the QD shape into consideration the initial local In-concentrations were corrected, resulting in an In-concentration profile in growth direction of about 50 % near the base of the QD which increases to almost 90 % at the top.

Acknowledgements This work has been performed within the project A2 of the DFG Research Center for Functional Nanostructures (CFN). It has been further supported by a grant from the Ministry of Science, Research and the Arts of Baden-Württemberg (AZ: 7713.14-300).

References

[1] O. B. Shchekin and D. G. Deppe, Appl. Phys. Lett. **80**, 3277 (2002).
[2] W. Löffler, D. Tröndle, J. Fallert, H. Kalt, D. Litvinov, D. Gerthsen, J. Lupaca-Schomber, T. Passow, B. Daniel, J. Kvietková, M. Grün, C. Klingshirn, and M. Hetterich, Appl. Phys. Lett. **88**, 062105 (2006).
[3] A. Rosenauer, W. Oberst, D. Litvinov, D. Gerthsen, A. Förster, and R. Schmidt, Phys. Rev. B **61**, 8276 (2000).
[4] M. A. Migliorato, A. G. Cullis, M. Fearn, and J. H. Jefferson, Phys. Rev. B **65**, 115316 (2002).
[5] M. Bissiri, G. Baldassarri Höger von Högersthal, M. Capizzi, P. Frigeri, and S. Franchi, Phys. Rev. B **64**, 245337 (2001).
[6] G. A. Narvaez, G. Bester, and A. Zunger, J. Appl. Phys. **98**, 043708 (2005).
[7] A. Rosenauer and D. Gerthsen, Ultramicroscopy **76**, 49 (1999).
[8] A. Strecker, J. Mayer, B. Baretzky, U. Eigenthaler, T. H. Gemming, R. Schweinfest, and M. Rühle, J. Electron Microsc. **48**, 235 (1999).
[9] P. Stadelmann, Ultramicroscopy **21**, 131 (1987).
[10] A. Rosenauer, M. Schowalter, F. Glas, and D. Lamoen, Phys. Rev. B **72**, 085326 (2005).
[11] K. Scheerschmidt, in: Theory of Defects in Semiconductors, edited by D.A. Drabold, S. Estreicher, Topics in Applied Physics 104, (Springer Verlag, Berlin – Heidelberg – New York, 2007), chap. 9.
[12] S. J. Pennycook, D. E. Jesson, A. J. McGibbon, and P. D. Nellist, J. Electron Microsc. **45**, 36 (1996).
[13] P. Wang, A. L. Bleloch, M. Falke, and P. J. Goodhew, Appl. Phys. Lett. **89**, 072111 (2006).
[14] D. M. Bruls, J. W. M. Vugs, P. M. Koenraad, H. W. M. Salemink, J. H. Wolter, M. Hopkinson, M. S. Skolnick, Fei Long, and S. P. A. Gill, Appl. Phys. Lett. **81**, 1708 (2002).

